Research Article

Journal of RAMAN SPECTROSCOPY

Received: 20 August 2009 Accepted: 9 May 2010 Published online in Wiley Online Library: 5 July 2010

(wileyonlinelibrary.com) DOI 10.1002/jrs.2723

Characterization of carbon nanotube filters and other carbonaceous materials by Raman spectroscopy – II: study on dispersion and disorder parameters

H. M. Heise,[a]* R. Kuckuk,[a] A. Srivastava[b] and B. P. Asthana[b]

Recently, we have reported on the characterization of various carbonaceous materials including multiwalled carbon nanotube (MWCNT) filters, which have specific molecular filtering capabilities and good mechanical strength and can be produced in bulk as highly aligned arrays of bundles of CNTs. We have extended our studies using Fourier transform-Raman spectroscopy with 1064 nm excitation wavelength and a rotating sample holder in the region 1000–2800 cm^{-1}, in addition to 532 and 785 nm, which were used for Raman excitation in our previous study. Raman spectra were analyzed for band positions and line shape with special emphasis on the D-, G- and G′- bands. For the single-walled species, Carbotrap and graphite spectra were also recorded with 488 nm excitation. A dispersion study has been made from the Raman data available with the different excitation wavelengths. Slight band shifts and band broadening could be observed under the two sample conditions, one with the stationary sample and the other with sample rotation. The spectral changes are related to the excessive heating caused in a stationary sample by laser irradiation. Based on our findings in this study combined with our earlier study, we can state that only a careful line shape analysis and study of intensity pattern of the D- and G-Raman bands under well-defined measurement conditions lends itself as a good measure of degree of alignment in the MWCNT bundles. Copyright © 2010 John Wiley & Sons, Ltd.

Keywords: carbon nanotube filters; carbonaceous materials; Raman spectroscopy; dispersion of D- and G′-bands; sample temperature effects

Introduction

Carbon is one of the most abundant elements in nature and exists in several forms depending upon its state of hybridization. These different forms range from simple graphite to diamond and from fullerenes to graphene and nanotubes with single and multiple walls with very distinct physical and chemical properties. Almost two decades ago, Iijima[1] reported the formation of helical microtubules of graphitic carbon, which was later named as carbon nanotube (CNT). There is much interest nowadays on the different uses of these materials for general applications in analytical science.[2] CNT-based transistors have been developed for biosensing as well as other sensor applications.[3–5] The review and the results presented by Hierold *et al*.[5] confirmed the potential and excellent performance of single-walled carbon nanotubes (SWCNTs) for sensors by the integration of the tubes in well-defined micro-electro-mechanical system (MEMS) structures. Recently Bokobza[6] performed mechanical, electrical and spectroscopic investigations of CNT-reinforced elastomers as composite materials, where matrices were filled with multiwalled carbon nanotubes (MWCNTs). These applications may illustrate the wide intrinsic potential of CNTs as novel materials.

The relationship of CNTs with other carbonaceous materials has recently been discussed by Dresselhaus and Endo.[7] Many different methods to grow CNTs have been reported in the literature and some most widely used techniques are arc discharge, laser furnace and chemical vapor deposition (CVD). Ando *et al*.[8] presented a review of these methods almost 5 years ago. Nearly contemporary to this review, a special MWCNT variety forming macroscopic hollow cylinders with radial alignment of its walls and having unique filtering capabilities and high mechanical strength was reported by Srivastava *et al*.[9] Recently, a scanning electron microscope (SEM) and Raman spectroscopic study of MWCNT grown by a novel technique on ash-supported catalysts was published.[10] Mono-dispersed SWCNTs made using an arc-burning method were described by Suzuki *et al*.[11]

Although there are many reviews and investigations on SWCNTs, see, for example, recent publications,[12–16] MWCNTs have less frequently been the subject of different studies. In our previous study on Raman spectra of various CNT varieties, i.e. SWCNTs and MWCNTs, graphitized porous carbon Carbotrap™ and graphite were recorded using excitation wavelengths of 532 and 785 nm,[17] and the results were analyzed in respect of peak positions, linewidths (FWHM, full width at half maximum) and intensities of the different component bands. The intensity ratios, I_D/I_G (I_D and I_G refer to the integrated intensities of D- and G-band

* *Correspondence to: H. M. Heise, Leibniz-Institut für Analytische Wissenschaften – ISAS – e.V. an der Technischen Universität Dortmund, D-44139 Dortmund, Germany. E-mail: heise@isas.de*

a *Leibniz-Institut für Analytische Wissenschaften – ISAS – e.V. an der Technischen Universität Dortmund, D-44139 Dortmund, Germany*

b *Department of Physics, Banaras Hindu University, Varanasi 221005, Uttar Pradesh, India*

peaks, respectively) were determined for two different MWCNT filter samples prepared using the method reported by Srivastava *et al*.,[9] and it was shown that this intensity ratio could be used as a sensitive parameter to monitor the degree of alignment in fully or partially aligned MWCNT bundles.

Recently DiLeo *et al*.[18] reported on purity assessment of MWCNTs prepared by CVD technique. The calibration curves with admixed nanostructured carbon were established for the Raman intensity ratios and the largest change was observed in the $I_{G'}/I_D$ ratio. It was concluded that the calibration curves obtained from relative Raman intensity ratios may be used as a viable means for MWCNT purity assessment. A comparative study of SWCNT purification technique using Raman spectroscopy has been communicated recently by Musumeci *et al*.[19] In another recent study,[20] the effect of intense laser on Raman modes of MWCNTs has been reported by varying the intensity of the incident laser radiation for Raman excitation. It has been claimed that the decrease in the disordered parameter (I_D/I_G) in laser-irradiated CNT shows a purification of the CNTs.

Although the present work was initially aimed only at extending our earlier study[17] using Fourier transform (FT)-Raman spectroscopy with a third excitation wavelength of 1064 nm, which led to spectral data only using a rotating sample holder, we also recorded Raman spectra with 488 nm excitation. In view of the interesting studies from other groups as mentioned above, we also performed our experiments under two experimental conditions as realized for 785 nm laser excitation wavelength, i.e. one keeping the sample stationary and the other with sample rotation using a rotating sample holder, which has an effect on sample temperature. Thermal emission is known that it can have a detrimental effect on the Raman spectra.[21,22]

In view of the foregoing discussion, when examining the different intensity ratios under the two conditions, namely with and without rotation, concerns of intensity calibration of CCD-based Raman spectrometers were raised, for which further information is given in Ref. [23]. Finally, combining the results of earlier work, where only two wavelengths, 532 and 785 nm, were used for Raman excitation, we also could include a study on the dispersion of D- and G-bands for various carbonaceous materials. Furthermore, it was noticed that the intensities of D-, G- and G′-Raman bands in different carbonaceous materials including MWCNT filters show differences when the sample is stationary or rotating and it would be interesting to investigate whether the temperature effect has a similar kind of influence on the Raman bands of MWCNTs as a variation in incident laser intensity as studied recently.[20]

Experimental

Macro-scale hollow carbon cylinders up to centimetres in diameter and several centimetres long consisting of MWCNTs with diameters ranging from 20 to 50 nm were synthesized using a continuous spray pyrolysis method, where sprayed ferrocene-derived Fe particles act as catalyst. The nanotubes grow in radial directions on the walls of removable silica tube templates, leading to the formation of freestanding and continuous hollow cylindrical carbon tubes whose details are given elsewhere.[9]

CNT materials for comparison were purchased from Aldrich (Milwaukee, WI, USA; see also Ref. [17]). One of the charges was produced from CarboLex, Inc. of Lexington (Kentucky, USA). The batch quantity (product # 519308) was of AP-grade with bundles of SWCNTs (10–200 individual nanotubes per bundle with average diameters of 1.2–1.5 nm, bundle length of ~20 μm; individual tube length of 2–5 μm). The purity of the AP-grade (as prepared) product ranged from 50% to 70% by volume. Major impurities were carbon nanospheres and carbon-encapsulated catalyst nanoparticles. A second SWCNT material (product # 636797), specified as SWCNT (Aldrich), had diameters of 1–2 nm as measured by high-resolution transmission electron microscopy (HRTEM) with purity as follows: amorphous carbon: ~3%; other nanotubes: ~40%; SWCNT >50% with an average diameter of 1.1 nm and a length of 0.5–100 μm. The MWCNT (# 636525), named here as MWCNT (Aldrich 1), was specified by the following dimensions: OD × ID × length = 10–20 nm × 5–10 nm × 0.5–200 μm; carbon content ≥95%. We also procured a second MWCNT material from Aldrich with the following dimensions: OD × ID × length = 30–50 nm × 5–15 nm × 0.5–200 μm; carbon content >95%–labeled as MWCNT (Aldrich 2), for which Raman spectra were recorded. As the spectra of the two batches did not show any significant differences, the data for one batch only are presented and further discussed. Other materials studied were pure graphite and Carbotrap™ 20/40 mesh from Supelco (Bellefonte, PA, USA).

Three dispersive spectrometers with different excitation wavelengths were used. One of them was an XY-Dilor Raman spectrometer (HORIBA Jobin Yvon GmbH) equipped with a confocal Raman microscope, a triple 0.5 m monochromator, a Nd : YAG laser from Spectra-Physics with frequency doubling (excitation wavelength 532 nm) and a liquid-N_2 cooled CCD from WRIGHT Instruments Ltd for detection (slit width of 100 μm with integration time of 1000 s, 25 spectral frame accumulations). The second spectrometer used in this study was a HoloSpec Raman spectrometer from Kaiser Optical Systems, Inc., equipped with a diode laser (λ = 785 nm) from SDL, Inc. and a liquid-N_2 cooled CCD detector from RS Roper Scientific (integration time, e.g. of 25 s with 10 spectral frame accumulations, laser power of 14 mW). Further measurements were carried out using a Raman spectrometer model Acton Tri-Vista from Princeton Instruments, equipped with a liquid-N_2 cooled CCD detector from RS Roper Scientific, and a Spectra-Physics Ar-Laser (wavelength of 488 nm).

The Fourier transform near-infrared (FT-NIR) Raman spectrometer model PE-2000 (Perkin-Elmer, Überlingen, Germany) comprises of a 2 W diode pumped Nd : YAG laser (IE Optomech Ltd, Newnham, UK) for NIR excitation (wavelength of 1064 nm) and a GaAs detector. The following experimental conditions were chosen for spectral recordings: spectral resolution of 16 cm^{-1} and 1000 interferogram scans were coadded at 100 mW of laser power to get the final spectra. Spectra of reasonable signal-to-noise ratio could only be obtained for graphite and SWCNT samples. For recording spectra of the other bulk materials, a rotating sample holder was used to reduce excessive sample heating from laser irradiation.

The spectra with 785 nm excitation were recorded for stationary samples as well as with sample rotation. For sample rotation, a mount was prepared out of a brass cylinder having 15-mm diameter and 7-mm height. At open face of this brass piece, a circular groove of 2-mm width (external and internal diameters 9 and 7 mm, respectively) and 1-mm depth was cut. The samples of the carbonaceous materials were filled in this circular groove and pressed with a brass press having the same dimension in order to ensure uniform distribution of the sample over the entire groove area. The sample holder could be rotated with 170–2500 revolutions per minute (rpm). The Raman scattered radiation from

the carbonaceous materials was collected with 180° scattering geometry.

Results and Discussions

Raman spectra and line shape analysis of different bands

Raman spectroscopy is an important tool for investigating such materials because their spectrum is particularly sensitive to the microstructure of the carbon. In the present study, the Raman spectra of different varieties of CNT along with other carbonaceous materials are reported for the region of 1000–2800 cm^{-1}. Our major emphasis in this study was on the MWCNT filter variety with regard to other materials. An SEM micrograph of aligned MWCNT filter is given in Fig. 1(a), which clearly shows the long CNTs and degree of their alignment. The nanostructure of the MWCNT filter tubes is illustrated by a TEM micrograph (Fig. 1(b)). A comparison of the Raman spectra of different carbonaceous materials recorded using different excitation wavelengths and sample conditions is presented in Fig. 2. It can be clearly seen that different excitation wavelengths not only alter appreciably the Raman peak positions but also change the intensity pattern of the different Raman bands significantly.

The spectra recorded using 488 nm excitation and a stationary sample holder are shown in Fig. 3(a); similarly, spectra obtained with stationary samples and 1064 nm excitation are displayed in Fig. 3(b). In the present study, in order to get better quality spectra with 1064 nm excitation, it was rather necessary to use a rotating sample holder for improving the quality of the spectra significantly. It was without difficulty to record also the low wavenumber region showing the radial breathing mode band that is observable in the spectra of single-walled nanotubes (SWNTs). For demonstrating the influence of sample rotation, a typical study was made in this work, where the spectra of two samples were recorded with varying sample rotation speed in the range of 550–2500 rpm. The spectra are presented in Fig. 4, and it is obvious that with increasing rotation speed, the spectral quality goes on improving.

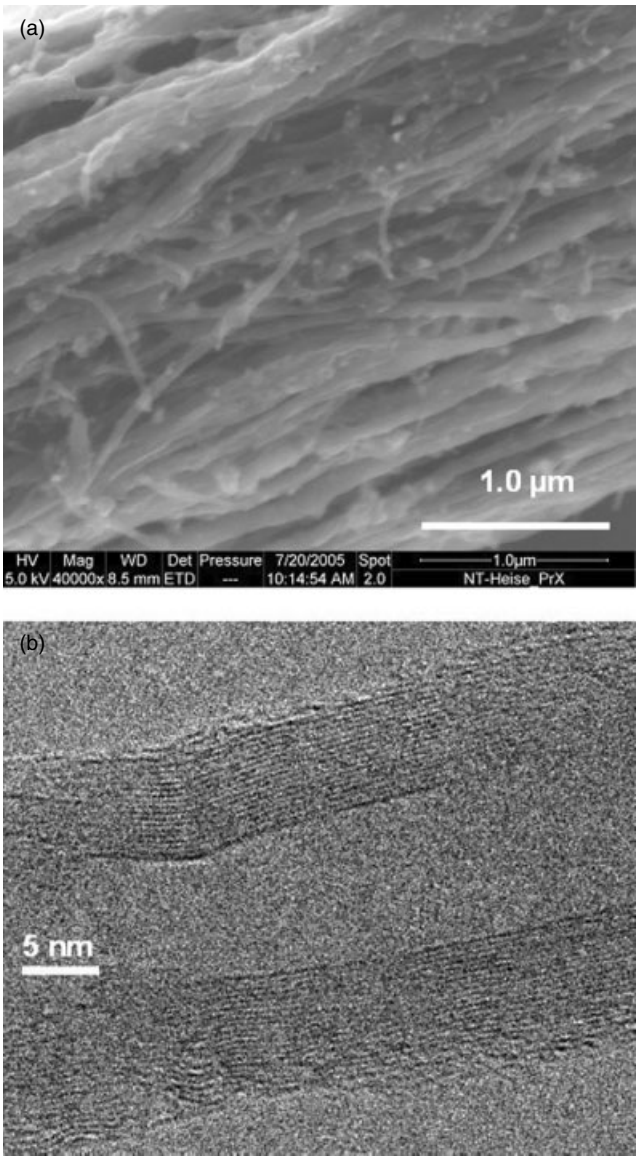

Figure 1. (a) SEM micrograph of aligned multiwalled carbon nanotubes (MWCNT filter); (b) HRTEM photograph of an isolated MWCNT of the same material.

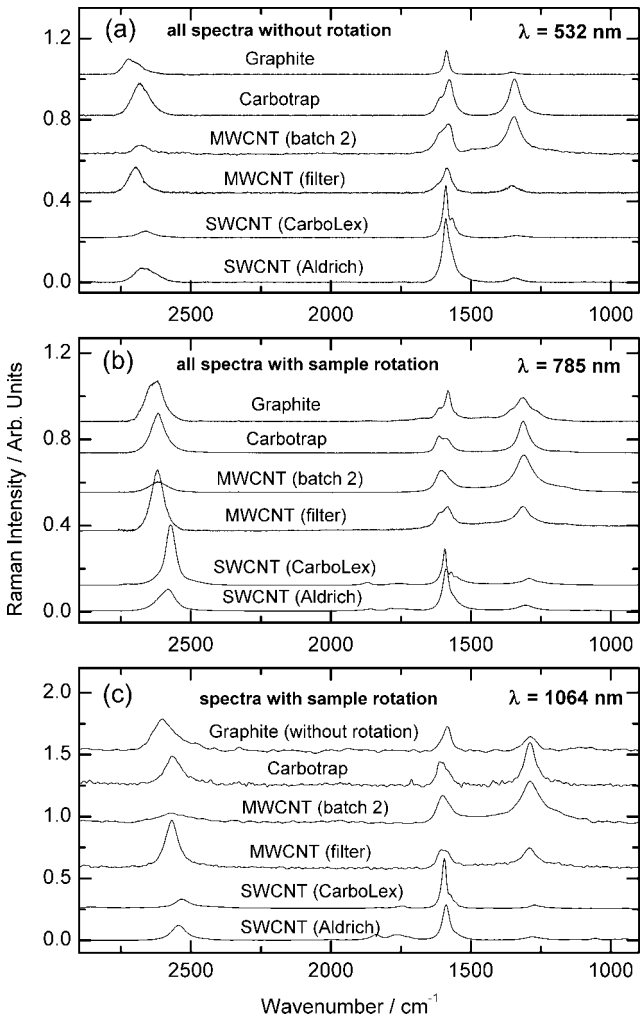

Figure 2. Comparison of the Raman spectra of different carbonaceous materials recorded using different excitation wavelengths and sample conditions: (a) spectra using 532 nm as excitation wavelength with a stationary sample; (b) spectra using 785 nm as excitation wavelength; (c) spectra using 1064 nm as excitation wavelength, the latter two measurement conditions were with sample rotation.

Journal of RAMAN SPECTROSCOPY

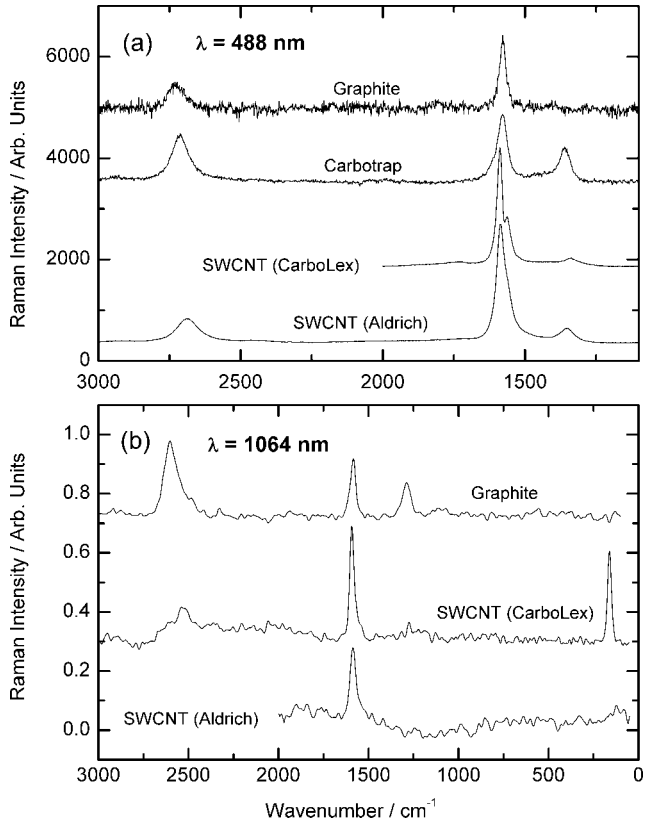

Figure 3. (a) Raman spectra obtained with 488 nm laser excitation wavelength; (b) FT-Raman spectra of the same carbonaceous materials without sample rotation and 1064 nm Raman excitation wavelength.

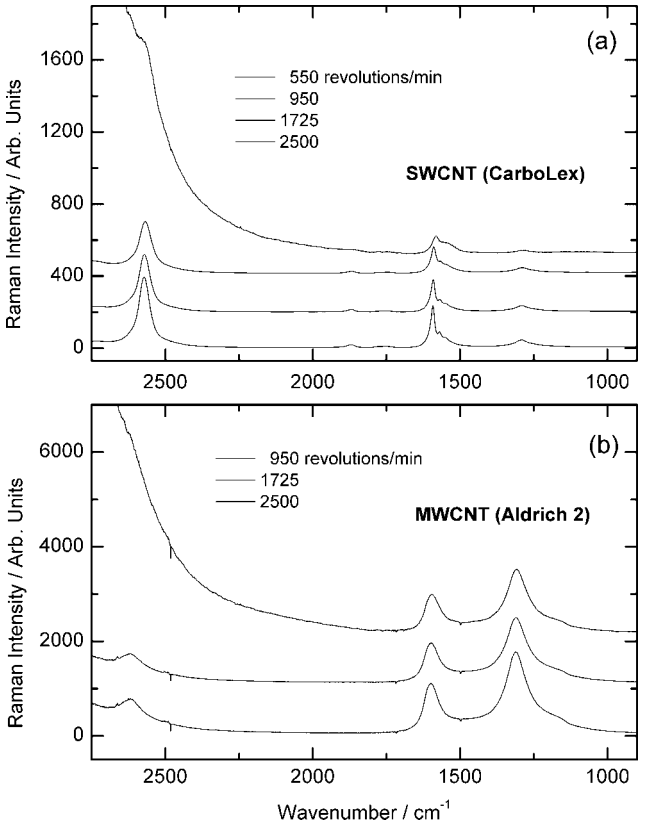

Figure 4. Raman spectra of two carbonaceous materials, SWCNT (CarboLex, Aldrich #519308) (a) and MWCNT (Aldrich 2 #636630) (b) using 785 nm excitation with sample rotation at varying rotation speed.

Furthermore, it is also seen clearly that with low sample rotation speed (<1000 rpm), some of the spectral features are not even observed.

A careful analysis of the spectra recorded under stationary and rotating sample holder shows that small differences in spectral features exist, which is exemplarily shown with spectra from three different samples recorded with 785 nm excitation wavelength (Fig. 5). Detailed results were obtained by band deconvolution using band fitting. The detailed analysis of the prominent bands in the Raman spectra for two different MWCNT varieties is presented in Fig. 6, where the D-, G- and G′-bands are analyzed for the component bands. The results of the band fitting procedures, using OPUS software from Bruker Optics (Ettlingen, Germany) and giving the peak position, linewidth (FWHM) and integrated band intensities, are presented in Table 1. Taking main results presented in Table 1 from all the samples, I_D/I_G and $I_D/I_{G'}$ ratios are presented in Table 2.

The band around ~1310 cm^{-1} (785 nm excitation), which is assigned as D-band with an asymmetric feature toward lower wavenumbers, gives rise to a weak component band at ~1180 cm^{-1}. This band is also evident in the MWCNT spectra recently shown by Kumar *et al*.[20] The linewidth of this weak band is larger than that of the main D-band. This is also supported by a detailed band analysis of the G- and D-band spectral region that was carried out for disordered structure materials such as coke carbon.[24] The D-peak arises as a result of resonant Raman coupling to the phonon excited by the incident photon (a double-resonance phenomenon). The dominant Raman intensity of the D-band can

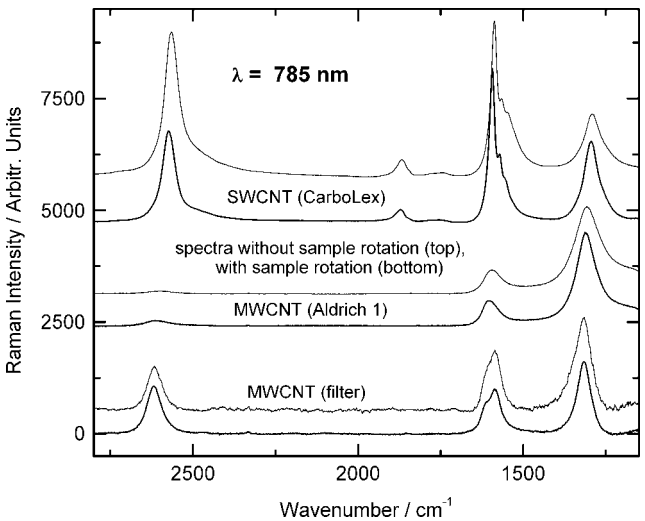

Figure 5. Comparison of the Raman spectra of different carbonaceous materials recorded with stationary sample and sample rotation using 785 nm as excitation wavelength: top spectra – SWCNT (CarboLex); middle spectra – MWCNT (Aldrich); bottom spectra – MWCNT filter.

normally be understood in terms of symmetric breathing modes of clusters of six-fold rings.

The peak around ~1585 cm^{-1}, which is assigned as G-band, shows a composite nature and it is fitted to two peaks for the MWCNT filter material (Fig. 6(a)). A rigorous line shape analysis

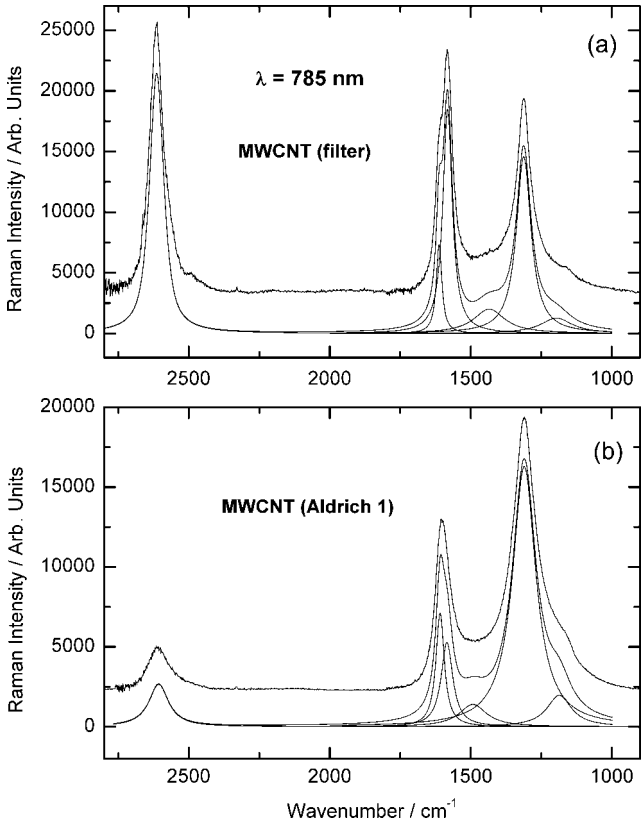

Figure 6. Comparison of the Raman spectra of two different MWCNT samples recorded with stationary sample using 785 nm as excitation wavelength: MWCNT (filter) (a) and MWCNT (Aldrich 1) (b); exemplarily, the measured line profiles have been deconvoluted into the component bands.

yields two bands at the wavenumber positions of 1583.6 cm^{-1}, originating from the Brillouin zone and being close to the graphite frequency of 1582 cm^{-1}, and 1615.2 cm^{-1} for MWCNT (filter) with 785 nm excitation and sample rotation (bands separated by 31.6 cm^{-1}; Table 1). The latter band (also called D′) is typical for defective graphite-like materials.[25,26] It has its origin from a nonzero wavevector and is based on the double-resonance phenomenon, consequently facing a different physical origin for both bands. The G-band complexity and nomenclature are different for SWCNT with G^+ and G^- components.

The G- peak originates due to sp^2 sites present in the sample, and this represents the ν(C═C) stretching vibration of all pairs of sp^2 atoms in both rings and chains. The composite peak nature and the shift are, in general, a consequence of nanotube curvature. This curvature results into deviation from sp^2 hybridization and consequently the C–C bonds along the axis of the tube and along the circumferential direction have different force constants, which in turn give rise to different vibrational wavenumbers for the ν(C═C) vibrations along the axis of the nanotube and in the circumferential direction.

The band around ~2610 cm^{-1} with 785 nm excitation in the spectra of MWCNTs is assigned to be G′-band. A recent study was concerned with a detailed analysis of the G′-band line shape in graphite foams.[27] It is to be noted that this band is also referred to as D*[28] – note the ambiguity with the nomenclature above – whereas other authors refer to it as G′-band, which we have followed in our earlier study,[17] and hence we will stick to

Table 1. Results from band fitting with band positions, bandwidths and band areas (for bands marked with an asterisk Gauss–Lorentz profile have been used, for others pure Lorentzian line functions were applied; band areas in arbitrary units)

	ν	$\Delta\nu$	Band area	N	$\Delta\nu$	Band area
	532 nm without rotation			1064 nm with rotation		
MWCNT (filter)	1352.3	44.3	2.47	1291	60	13.9
	1585.0	31.9	6.09	1587	40	6.9
	1616.9	31.0	1.11	1609	24	3.5
	2697.1	59.1	9.18*	2568	53.5	32.2
MWCNT (Aldrich 1)	1346.3	64.2	17.64	1288	85.5	42.5
	1578.5	26.2	5.02	1581	45	7.5
	1608.2	41.1	5.89	1605	31	7.9
	2677.0	60.6	3.58*	2561	105.5	11.1
Carbotrap	1343.6	40.8	11.70	1288	49	26.9
	1577.4	31.1	8.52	1590	35.5	6.9
	1610.3	26.1	2.39	1611	22	5.2
	2679.4	74.8	12.99*	2563	67.5	24.6
Graphite	1353.4	37.0	0.62	1288	56	6.7*
	1587.1	18.8	3.53	1586	39	7.7*
	2692.7	53.1	3.75	2547	148	12.6*
	2725.7	34.0	3.23	2606	74	15.9*
SWCNT (CarboLex)	1334.4	48.5	0.81	1270	51	2.1
	1563.4	18.3	1.75	1557	17	0.7
	1590.5	20.0	7.74	1571	9	0.7
	2662.5	65.6	3.24*	1595	20	12.4
				2463	145	1.3
				2532	53	5.5
SWCNT (Aldrich)	1342.3	45.8	1.58	1277	73	3.1
	1569.9	40.0	5.98	1548	36	1.2
	1590.4	25.0	10.38	1589	29	13.2
	2642.3	64.3	4.43	2543	62	11.0*
	2681.0	49.2	4.08			
	785 nm without rotation			785 nm with rotation		
MWCNT (filter)	1197.4	155.2	1.73	1223.3	175.2	2.25
	1312.2	62.0	7.44	1314.2	59.0	7.83
	1432.0	147.8	2.45	1427.8	187.3	5.19
	1582.3	40.5	6.18	1583.6	42.4	5.93
	1612.4	24.1	1.45	1615.2	26.3	1.70
	2613.9	55.9	10.15*	2619.6	54.5	18.80
MWCNT (Aldrich 1)	1185.6	105.4	3.01	1193.5	109.1	2.69
	1310.3	100.2	23.32	1310.4	75.3	19.60
	1493.1	125.0	2.71	1485.1	124.0	2.11
	1585.1	50.4	3.87	1586.6	47.0	4.12
	1609.0	35.8	3.55	1610.5	30.8	3.30
	2606.4	84.6	3.18	2616.1	66.2	5.14
Carbotrap	1167.5	79.0	0.52	1169.4	52.4	0.34
	1310.0	46.9	10.42	1312.7	45.8	10.41
	1591.9	42.4	4.07	1586.3	38.0	3.55
	1610.5	25.1	2.32	1614.8	22.5	2.15
	2608.4	62.2	7.50	2617.4	60.6	14.56*
Graphite	1313.6	47.8	5.47	1314.8	57.8	9.32
	1581.9	19.1	5.42	1581.5	26.9	5.42
	1613.1	15.9	0.42	1614.3	23.8	1.46
	2616.4	63.1	4.67	2610.9	55.0	8.75*
	2651.8	38.3	3.48	2643.3	59.3	7.80*

Journal of RAMAN SPECTROSCOPY

Table 1. (*Continued*)

	ν	$\Delta\nu$	Band area	N	$\Delta\nu$	Band area
	785 nm without rotation			785 nm with rotation		
SWCNT (CarboLex)	1287.5	82.2	4.50	1289.3	77.7	3.84
	1547.1	52.0	5.60	1550.7	34.0	2.60
	1564.5	11.5	0.36	1570.1	16.6	1.72
	1589.8	20.5	5.57	1593.1	17.1	4.69
	2567.7	47.8	24.8	2571.7	44.5	21.6
SWCNT (Aldrich)	1301.6	70.7	2.55	1304.6	66.5	2.58
	1552.4	54.7	3.10	1556.6	48.2	2.39
	1584.7	27.3	7.92	1588.9	27.1	7.92
	2577.7	72.8	4.51	2577.9	50.4	6.89
				2610.5	51.1	3.05

Table 2. Intensity ratios, I_D/I_G and $I_D/I_{G'}$ for different materials calculated from the integrated Raman intensities of the individual band components obtained from line shape analysis reported in Table 1 for the Raman excitation wavelength of 785, 532 and 1064 nm with different sample recording conditions

Name of the sample	Without sample rotation		With sample rotation	
	I_D/I_G	$I_D/I_{G'}$	I_D/I_G	$I_D/I_{G'}$
	785 nm[a]			
MWCNT (filter)	0.98	0.73	1.03	0.42
MWCNT (Aldrich 1)	3.14	7.33	2.64	3.81
Carbotrap	1.63	1.39	1.83	0.71
Graphite	0.94	0.67	1.35	0.56
SWCNT (CarboLex)	0.39[b]	0.18[b]	0.43	0.18
SWCNT (Aldrich)	0.23	0.57	0.25	0.26
	532 nm		1064 nm	
MWCNT (filter)	0.34	0.27	1.33	0.43
MWCNT (Aldrich 1)	1.62	4.93	2.75	3.83
Carbotrap	1.07	0.90	2.72	1.09
Graphite	0.18	0.09	0.87	0.23
SWCNT (CarboLex)	0.085	0.25	0.15	0.30
SWCNT (Aldrich)	0.097	0.18	0.21	0.28

[a] For the spectra recorded with 785 nm without sample rotation, a different CCD intensity correction had been applied compared to conditions with a nonstationary sample.
[b] Ratios calculated from spectrum with same CCD intensity correction as with sample rotation.

this nomenclature also here. For SWCNT, the G′-band appeared around ~2600 cm^{-1}, often with two band components. This band is known as the overtone band of the D-band. The wavenumber of the disorder-induced D-band and of its second-order overtone G′-band in the Raman spectra of sp^2 bonded carbon materials have been known for many years to exhibit a strong dispersive behavior as a function of the laser excitation energy.[17] The physical origin of the D- and G′-band features in the Raman spectra in isolated CNT as well as in MWCNTs is based on the double-resonance mechanism. The double-resonance effect in graphite occurs when both initial and final states, as well as the intermediate scattering states are actually electronic states.

Dispersion of D- and G-bands

In our earlier study,[17] Raman D-band and degree of alignment were the major points of emphasis. With only two wavelengths, i.e. 532 and 785 nm in the previous study, there were no sufficient data for determining the wavelength dependency of the dispersion effect by least squares. As the study has been extended taking into account further excitation wavelengths, 488 and 1064 nm, we are able to discuss the dispersion in the different carbonaceous materials in more detail. The change in the peak position of the D-band with excitation wavelength has been explained in literature in terms of resonance of electronic and vibrational density of states. It has been observed in carbonaceous materials that when phonon wavenumbers vary with a change in excitation wavelength,[29–32] a weak Raman signal is observed. In the present study, the spectra are recorded under two different sample conditions, one with stationary sample and the other with sample rotation. It can be seen from the spectra presented in Fig. 5 that there is a slight difference in the band shapes and band shifts under two sample conditions (spectra had been measured one after another and displayed without CCD detector intensity correction). This aspect will, however, be discussed in a forthcoming section, where the implications of the intensity variation of the incident laser used for Raman excitation shall be discussed in more detail.

The dispersion of the Raman D-band is quite obvious if the data presented in Table 1 is examined. The first part of the table contains data of analyzed Raman peaks with 532 nm excitation without rotation of the sample and 1064 nm excitation with sample rotation. The second part of the table contains the data of analyzed Raman peaks with 785 nm excitation under both sample conditions. The Raman D-band shows a shift of ~2 cm^{-1} between the spectra recorded with sample rotation and without sample rotation using 785 nm excitation for the MWCNT filter (Table 1), whereas the difference is more pronounced in the SWCNT samples studies (4.2 and 5.9 cm^{-1}, respectively). If we compare the Raman peaks corresponding to D-band for all the three excitations, e.g. for MWCNT filter, the D-peaks are observed at 1352.3, 1314.2 and 1290.8 cm^{-1} for 532, 785 and 1064 nm excitations, respectively. Band positions are summarized in Table 3, which also contains spectral data obtained with 488 nm excitation wavelength. The data for all materials studied are graphically presented in Fig. 7(a), illustrating clearly a similar excitation wavelength dependency for all samples.

The wavenumbers of the D- and G′-bands, the different excitation wavelengths and the corresponding energy values in eV are presented in Table 3. The calculated G′-band positions are twice the D-band wavenumbers, though experimental values have been observed at lower values. This phenomenon has been explained for the Stokes Raman spectra in graphite by Cançado *et al.*[33] using double-resonance mechanisms, whereas the D-band overtone (G′-band) in anti-Stokes spectra has been shifted to larger wavenumbers than $2\omega_D$. From the spectral data presented in this table, the dispersions of the D- and G′-bands were calculated for each material by a linear least squares fit taking the band positions *versus* the corresponding photon excitation energy (in eV) into account as illustrated in Fig. 7. In multiwalled nanotubes and graphite, the second-order peaks around 2695 cm^{-1} are attributed to a two-phonon process of the D-line at ~1350 cm^{-1} (532 nm excitation wavelength) as reported in earlier studies.[34,35] Kastner *et al.*[35] reported dispersion values for MWCNTs of 43 cm^{-1} eV^{-1} for the D-band and 89 cm^{-1} eV^{-1} for G′-band (excitation wavelengths between 457 and 676 nm). Our

Table 3. Wavenumbers of the D- and G′- bands of carbonaceous materials studied with four different Raman excitation wavelengths (488 nm ↔ 2.541 eV, 532 nm ↔ 2.330 eV; 785 nm ↔ 1.579 eV; 1064 nm ↔ 1.165 eV) along with the energy-dependent dispersion from the slope of a least squares fitted straight line

			Wavenumbers (cm^{-1})		
			D-band	G′-band	
Material	Excitation wavelength (in nm)	Dispersion cm^{-1} eV^{-1} for D and G′ bands		Experimental	Calculated[a]
MWCNT (filter)	532		1352.3	2697.1	2704.6
	785	52.7 ± 1.3	1314	2613	2628
	1064	109.9 ± 4.0	1291	2568	2582
MWCNT (Aldrich 1)	532		1346.3	2677.0	2692.6
	785	49.4 ± 1.2	1310.4	2611.3	2620.8
	1064	97.1 ± 9.2	1288.3	2561.4	2576.6
Carbotrap	488		1360.9	2714.5	2721.8
	532	49.8 ± 2.7	1343.6	2679.4	2687.2
	785		1311.4	2612.9	2622.8
	1064	104.2 ± 6.5	1288.4	2562.6	2576.8
Graphite	488			2731.0	
	532	55.2 ± 2.4	1353.4	2709.2	2706.8
	785		1314.2	2630.6	2628.4
	1064	110.1 ± 4.5	1288.3	2576.2	2576.6
SWCNT (CarboLex)	488		1341.9		
	532	53.4 ± 1.5	1334.4	2662.5	2668.8
	785		1292.4	2568.8	2584.8
	1064	114.2 ± 9.4	1269.7	2532.2	2539.4
SWCNT (Aldrich)	488		1352.5	2691.5	2705.0
	532	54.2 ± 2.0	1342.3	2661.7	2684.6
	785		1303.1	2582.7	2606.2
	1064	107.2 ± 4.8	1276.7	2543.1	2553.4

[a] The calculated G′-band positions are twice the D-band wavenumbers, see also text for further discussion.

values for MWCNT varieties are 49.4±1.2 and 97.1±9.2 cm^{-1} eV^{-1} for D- and G′-band, respectively. The dispersions for the D- and G′-bands for the MWCNT (filter) material turn out to be 52.7 ± 1.3 and 110 ± 4 cm^{-1} eV^{-1}, respectively. We noticed also differences for graphite (55.2±2.4 cm^{-1} eV^{-1} for D-band), which is larger than those values reported earlier (for graphite ≈50 cm^{-1} eV^{-1}[29]).

Thomsen[28] extended these measurements to SWCNTs and found similar results and concluded on the basis of his measurements that D and G′ (his nomenclature D*) lines in SWNT shift with the excitation wavelength at the rate of 38 ± 2 and 90 ± 3 cm^{-1} eV^{-1}, respectively. Our values for SWCNT materials are found to be much larger (54 ± 2 and 112 ± 7 cm^{-1} eV^{-1}) and are in better agreement with earlier studies by Pimenta *et al*. (respective values 53 and 106 cm^{-1} eV^{-1}).[36] Thus, the dispersions of both D- and G′-bands in the case of aligned MWCNT bundles (filter variety) are similar to our SWCNT values, much higher in comparison with those for SWCNT as reported by Thomsen,[28] covering the range of 1.9 up to 2.8 eV for his excitation energy dependence study of the D- and G′-bands. When the large wavelength range is considered, the excitation energy-dependency is nearly the same for all studied carbonaceous materials studied here (see also Table 3).

A comment is appropriate for the SWCNT materials, because the mode characteristics provide information on the SWCNT electronic properties (metallic or semiconducting), as well as on their structural disorder.[25,37] Furthermore, the dispersive disorder-induced D-mode is not only associated with the double-resonance effects but also dependent on the average tube diameter.[38] The data show that G′- and D-band frequencies of both SWCNT varieties are lower than for the other carbon species, which is due to curvature effects on the D-band. This is further confirmed by inspecting the Aldrich *versus* Carbolex data. The SWCNT (Aldrich) sample has an average diameter measured by HRTEM larger than that of the Carbolex material; consequently, the D and G′ frequencies follow the expected diameter dependence as discussed in Ref. [38]. Using the linear relationship as given for D-band data that was obtained for the 785 nm laser excitation wavelength and an average diameter of 1.35 nm for the Carbolex SWCNT material, the predicted band position is 1295 cm^{-1} (experimental value 1292.4 cm^{-1}). Using the same function and the D-band wavenumber of the Aldrich SWCNT material, a too large diameter of 3 nm is calculated. However, if our graphite D-band position of 1314.2 cm^{-1} – slightly higher than the frequency of 1309 cm^{-1} as reported by Souza Filho *et al*.[38] – is taken into account, a diameter value of 1.7 nm follows, which agrees with a plausible HRTEM average value that is in contrast to the given average diameter reported by the distributor. The suitability of the Raman spectrum for the determination of structural parameters is demonstrated.

Disorder and purity of the carbonaceous materials

In our earlier study,[17] we reported in detail on the characterization of various carbonaceous materials including a special variety of MWCNT bundles.[9] It was shown that I_D/I_G ratio of the Raman intensities for a given sample is strongly dependent on the laser

Journal of RAMAN SPECTROSCOPY

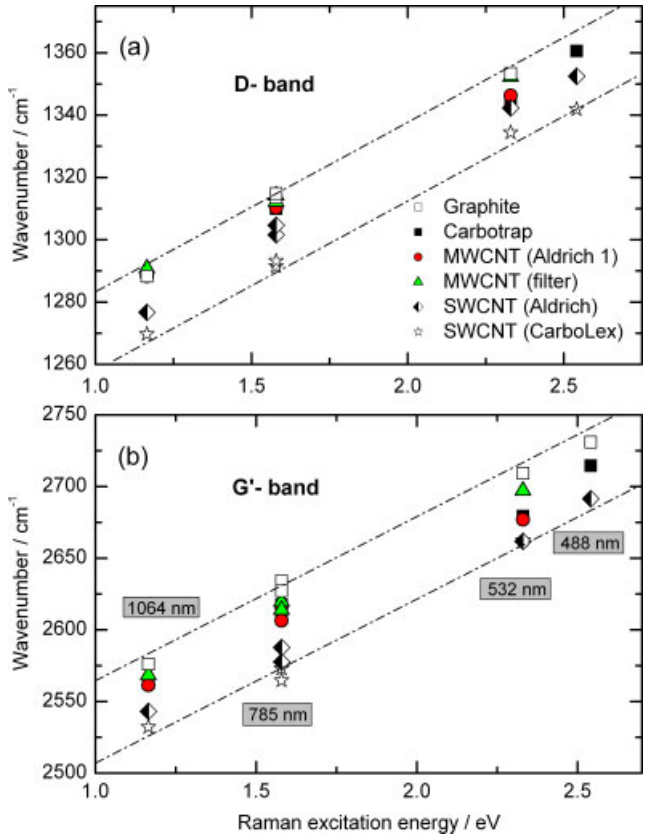

Figure 7. Dispersion of Raman D- (a) and G′-bands (b) of different carbonaceous materials for mainly four excitation wavelengths, 488, 532, 785 and 1064 nm with the abscissa in eV; the bands enclosed by the dash-dotted lines suggest a linear dependency of the band shifts on the excitation energy.

energy, but did not follow the E^{-4}_{laser} type dependence as reported through an optical study on CNTs and nanographites by Pimenta *et al*.[39] This E^{-4} dependence was found for the nanographite material and refers to the photon energy E of the excitation wavelength, while it does not take into account the intensity of the laser radiation used for Raman excitation. For studying spectral intensities, especially recorded by different spectrometers, a relative intensity correction using standard reference materials[23] becomes essential. However, it is quite natural to assume that there will be some influence of the incident laser intensity on the general spectral features as pointed out by other authors.[21,22] Spectral baseline effects were much reduced with high rotation speed of the sample holder, allowing more accurate band intensity integrations. Because of the missing spectrometer intensity calibrations, the dependency of I_D/I_G on the laser excitation energies was not further elaborated, although the ratio has been suggested for quality assessment and production control.[17,40]

Previously,[17] two excitation wavelengths, i.e. 532 and 785 nm, were used by us for recording the Raman spectra. In the present work, however, when the study was extended taking 1064 nm as excitation wavelength and the attempts were made to record the Raman spectra, it was observed that in certain cases, the spectra were of rather poor quality. A typical example of the Raman spectra recorded without sample rotation is presented in Fig. 3(b). Recently DiLeo *et al*.[18] made a detailed study on purity assessment of MWCNTs by Raman spectroscopy. In their Raman study, calibration curves based on I_D/I_G, $I_{G'}/I_G$ and $I_{G'}/I_D$ ratios were given, and it was concluded that these calibration curves could be used for quantitative purity assessment. Earlier this group had done a similar work on purity assessment of SWCNTs using optical absorption spectroscopy.[41]

Recently, Raman spectroscopy has been exploited to investigate even the mechanical and electrical properties of CNT-based elastomers.[6] In another recent study defect-dependent annealing behavior of MWCNTs was studied by Bhalerao *et al*.,[42] where I_D/I_G was used as an important parameter to examine the effect of annealing. The annealing of MWCNTs was carried out in hydrogen atmosphere at temperatures $<1300\,^{\circ}C$. Thus, it appears that I_D/I_G has been used for studying many different properties of SWCNTs and MWCNTs.

A more controversial study has been published recently by Kumar *et al*.[20] who studied the effect of intense laser and energetic ion irradiation on Raman modes of MWCNTs. Samples had been irradiated by a 514 nm Ar ion laser with a maximum laser power of 50 mW and with fractions of this, i.e. 0.5, 1.0, 2.5, 5.0, 12.5 and 25 mW. The authors noticed quite some drastic changes in band position for the D and G modes in the range up to 10 cm^{-1}. In addition to this, the I_D/I_G ratio was monitored with the integral intensities obtained by Lorentz band fitting. Although the G-mode band position behavior was fully reversible, the D-mode shifts did not completely recover after sample exposure to maximum laser power when recorded again with lower laser power (spectral shift compared with the band position recorded with a fresh sample 4 cm^{-1}). The intensity ratio also remained constant after maximum sample irradiation ($I_D/I_G = 1.5 \pm 0.1$), indicating some purification or ordering in MWCNTs, possibly with a burn out of amorphous carbon in air as suggested also by other authors. We studied temperature effects with exposure to 15 mW laser power, but applying different sample rotation frequencies.

When we started with a revolution frequency of 2500 rpm, band positions were highest for MWCNT (Aldrich 2) samples (1310.3 and 2615.7 cm^{-1} for D-band and G′-band positions, respectively, whereas halving the revolution frequency moved those wavenumbers to 1308.7 and 2612.4 cm^{-1} (the band position of the G-band was shifted only marginally by 0.6 cm^{-1}). Intensity ratios I_D/I_G increased slightly from 3.8 to 3.9 for the higher temperature sample at lower revolution frequency. Similar results for the band shifts have been obtained for the SWCNT (CarboLex) sample: the D- and G′-band positions were shifted from 1289.3 and 2571.7 cm^{-1} under 2500 rpm to 1287.5 and 2567.7 cm^{-1} with ~900 rpm, respectively. Here the G-band position changed more noticeably from 1593.1 to 1589.8 cm^{-1}. On the other hand, the intensity ratio I_D/I_G changed from 0.43 to 0.39 for the higher temperature sample at lower revolution frequency, indicating possibly some very minor purification if such interpretation is permitted.

On the basis of the results on I_D/I_G determined in our earlier study[17] as well as both I_D/I_G and $I_{G'}/I_G$ in the present study, we have arrived at the conclusion that it is probably an over-simplification and over-emphasis to make a quantitative purity assessment based on Raman intensity ratios, especially in the case of MWCNTs. In fact, by combining the results of our previous and the present study, we have been able to demonstrate that both I_D/I_G and $I_D/I_{G'}$ ratios can tell more clearly about the degree of order and alignment in the MWCNT bundles. For the 785 nm Raman excitation, it seems that the intensity calibration for the sample rotation conditions had amplified the G′-band intensities by a factor of two. This clearly points out the necessity of using

standard reference materials for checking the correct Raman intensities over a broad spectral range.

From the results presented above and foregoing discussions, it is evident that under sample rotation condition, when a fresh location of the sample is always exposed to the incident laser radiation, the spectral quality is much better. Under a stationary sample condition, it is obvious also from the band broadening that there is an excessive heating of the sample due to resonant absorption of the incident laser radiation. On the basis of the results obtained in this study, we have arrived at the conclusion that sample rotation for bulk samples, even if not an absolute necessity, is definitely a better option for recording the Raman spectra of SWCNTs and MWCNTs in order to get a better spectral quality.

Conclusions

A dispersion study of both D- and G′(D*)-bands of the MWCNT (filter) was made using the data obtained from the Raman measurements taking three different excitation wavelengths, namely 532, 785 and 1064 nm, into account. The dispersion of D- and G′-bands evaluated from the wavenumber positions obtained through line shape analysis of the experimental profiles turned out to be 52.7 ± 1.3 and $109.9 \pm 4.0\ cm^{-1}\ eV^{-1}$ (energy of the incident photon), respectively, which are significantly different and higher as compared with what was reported for SWCNT and other carbonaceous materials based on smaller changes in Raman excitation wavelengths. For other materials, also spectral data obtained with 488 nm excitation wavelength was available. A significant result of this study was an obvious enhancement in the overall spectral quality with regard to baseline and intensity of all the three major features, namely D-, G- and G′-bands, when the sample was rotated as compared with the observed intensity with a stationary sample. In conclusion, our findings from this study together with our earlier study demonstrate that a careful line shape analysis along with the intensity pattern of the D- and G-Raman bands measured under well-defined conditions may lend itself as a tool to measure the degree of alignment in the MWCNT bundles.

Acknowledgements

B. P. A. would like to thank the Alexander von Humboldt-Stiftung for supporting his several visits, which formed the basis to initiate this collaborative effort. The authors from ISAS gratefully acknowledge the financial support given by the North Rhine-Westphalia Ministry for Innovation, Science and Research and the Federal Ministry for Education and Research.

References

[1] S. Iijima, *Nature (London)* **1991**, *354*, 56.
[2] M. Valcarcel, B. M. Simonet, S. Cardenas, B. Suarez, *Anal. Bioanal. Chem.* **2005**, *382*, 1783.
[3] G. Gruner, *Anal. Bioanal. Chem.* **2006**, *384*, 322.
[4] N. Sinha, J. Ma, J. T. W. Yeow, *J. Nanosci. Nanotechnol.* **2006**, *6*, 573.
[5] C. Hierold, A. Jungen, C. Stampher, T. Helbling, *Sens.Actuators* **2007**, *A 136*, 51.
[6] L. Bokobza, *Vib. Spectrosc.* **2009**, *51*, 52.
[7] M. S. Dresselhaus, M. Endo, Relation of carbon nanotubes to other carbon materials, in *Carbon Nanotubes*, Topics in Applied Physics, Vol. 80 (Eds: M. S. Dresselhaus, G. Dresselhaus, Ph. Avouris), Springer-Verlag: Berlin, **2001**, 11.
[8] Y. Ando, X. Zhao, T. Sugai, M. Kumar, *Mater. Today* **2004**, (October issue), 22.
[9] A. Srivastava, O. N. Srivastava, S. Talapatra, R. Vajtai, P. M. Ajayan, *Nat. Mater.* **2004**, *3*, 610.
[10] G. M. Bhalerao, S. Waugh, A. Ingale, A. K. Sinha, M. Babu, P. Tiwari, R. V. Nandedkar, *J. Nanosci. Nanotechnol.* **2007**, *7*, 1860.
[11] S. Suzuki, T. Mizusawa, T. Okazaki, Y. Achiba, *Eur. Phys. J. D* **2009**, *52*, 83.
[12] M. S. Dresselhaus, G. Dresselhaus, R. Saito, A. Jorio, *Phys. Rep.* **2005**, *409*, 47.
[13] E. B. Barros, A. Jorio, G. G. Samsonidze, R. B. Capaz, A. G. Souza Filho, J. Mendes Filho, G. Dresselhaus, M. S. Dresselhaus, *Phys. Rep.* **2006**, *431*, 261.
[14] M. S. Dresselhaus, G. Dresselhaus, M. Hofmann, *Vib. Spectrosc.* **2007**, *45*, 71.
[15] A. Jorio, E. Kauppinen, A. Hassanien, Carbon-nanotube metrology, in *Carbon Nanotubes*, Topics in Applied Physics, Vol. 111 (Eds: A. Jorio, G. Dresselhaus, M. S. Dresselhaus), Springer-Verlag: Berlin, **2008**, 63.
[16] K. Yanagi, Y. Miyata, T. Tanaka, S. Fujii, D. Nishide, H. Kataura, *Diam. Relat. Mater.* **2009**, *18*, 935.
[17] H. M. Heise, R. Kuckuk, A. K. Ojha, A. Srivastava, V. Srivastava, B. P. Asthana, *J. Raman Spectrosc.* **2009**, *40*, 344.
[18] R. A. DiLeo, B. J. Landi, R. P. Raffaelle, *J. Appl. Phys.* **2007**, *101*, 064307.
[19] A. W. Musumeci, E. R. Waclawik, R. L. Frost, *Spectrochim. Acta A* **2008**, *71*, 140.
[20] A. Kumar, F. Singh, P. M. Koinkar, D. K. Avasthi, J. C. Pivin, M. A. More, *Thin Solid Films* **2009**, *517*, 4322.
[21] B. Schrader, A. Hoffmann, S. Keller, *Spectrochim. Acta A* **1991**, *47*, 1135.
[22] B. T. Bowie, D. B. Chase, P. R. Griffiths, *Appl. Spectrosc.* **2000**, *54*, 200A.
[23] S. Choquette, *Am. Lab.* **2005**, *37*, 22.
[24] M. Kawakami, H. Kanba, K. Sato, T. Takenaka, S. Gupta, R. Chandratilleke, V. Sahajwalla, *ISIJ Intern.* **2006**, *46*, 1165.
[25] A. Jorio, M. A. Pimenta, A. G. Souza Filho, R. Saito, G. Dresselhaus, M. S. Dresselhaus, *New J. Phys.* **2003**, *5*, 139.
[26] C. Thomsen, S. Reich, Raman scattering in carbon nanotubes, in *Light Scattering in Solid IX*, Topics in Applied Physics, Vol. 108, (Eds: M. Cardona, R. Merlin), Springer-Verlag: Berlin, **2007**, 115.
[27] E. B. Barros, A. G. Souza Filho, H. Son, M. S. Dresselhaus, *Vib. Spectrosc.* **2007**, *45*, 122.
[28] C. Thomsen, *Phys. Rev. B* **2000**, *61*, 4542.
[29] C. Thomsen, S. Reich, *Phys. Rev. Lett.* **2000**, *85*, 5214.
[30] M.J. Matthews, M.A. Pimenta, G. Dresselhaus, M.S. Dresselhaus, M. Endo, *Phys.Rev. B* **1999**, *59*, R6585.
[31] J. Kürti, V. Zólyomi, A. Grüneis, H. Kuzmany, *Phys. Rev. B* **2002**, *65*, 165433.
[32] R. Saito, A. Jorio, G. Souza Filho, G. Dresselhaus, M. Dresselhaus, M.A. Pimenta, *Phys. Rev. Lett.* **2001**, *88*, 027401.
[33] L.G. Cançado, M.A. Pimenta, R. Saito, A. Jorio, L.O. Ladeira, A. Grueneis, A.G. Souza-Filho, G. Dresselhaus, M.S. Dresselhaus, *Phys. Rev.* **2002**, *B66*, 035415.
[34] R.P. Vidano, D.B. Fischbach, L.J. Willis, T.M. Loehr, *Solid State Commun.* **1981**, *39*, 341.
[35] J. Kastner, T. Pichler, H. Kuzmany, S. Curan, W. Blau, D.N. Weldon, M. Delamesiere, S. Draper, H. Zandbergen, *Chem. Phys. Lett.* **1994**, *221*, 53.
[36] M.A. Pimenta, E.B. Hanlon, A. Marucci, P. Corio, S.D.M. Brown, S.A. Empedocles, M.G. Bawendi, G. Dresselhaus, M.S. Dresselhaus, *Brazilian J. Phys.* **2000**, *30*, 423.
[37] R. Saito, A. Grüneis, Ge G. Samsonidze, V.W. Brar, G. Dresselhaus, M.S. Dresselhaus, A. Jorio, L.G. Cançado, C. Fantini, M.A. Pimenta, A.G. Souza Filho, *New J. Phys.* **2003**, *5*, 157.
[38] A.G. Souza Filho, A. Jorio, Ge G. Samsonidze, G. Dresselhaus, M.A. Pimenta, M.S. Dresselhaus, A.K. Swan, M.S. Ünlü, B.B. Goldberg, R. Saito, *Phys. Rev.* **2003**, *B67*, 035427.
[39] M.A. Pimenta, A.P. Gomes, C. Fantini, L.G. Cançado, P.T. Araujo, I.O. Maciel, A.P. Santos, C.A. Furtado, V.S.T. Pressinotto, F. Plentz, A. Jorio, *Physica E* **2007**, *37*, 88.
[40] E.F. Antunes, A.O. Lobo, E.J. Corat, V.J. Trava-Airoldi, *Carbon* **2007**, *45*, 913.
[41] B.J. Landi, H.J. Raf, C.M. Evans, C.D. Cress, R.P. Raffaelle, *J. Phys. Chem. B* **2005**, *109*, 9952.
[42] G. Bhalerao, A.K. Sinha, V. Sathe, *Physica E* **2008**, *41*, 54.